Biochimica et Biophysica Acta 1838 (2014) 2588–2599

Contents lists available at ScienceDirect

Biochimica et Biophysica Acta

journal homepage: www.elsevier.com/locate/bbamem

Interactions of caveolin-1 scaffolding and intramembrane regions containing a CRAC motif with cholesterol in lipid bilayers

Guanhua Yang [a], Haoran Xu [b], Zhengqiang Li [b], Fei Li [a,*]

[a] State Key Laboratory of Supramolecular Structure and Materials, Jilin University, Changchun, 130012, PR China
[b] Key Laboratory for Molecular Enzymology & Engineering, The Ministry of Education, Jilin University, Changchun 130012, PR China

ARTICLE INFO

Article history:
Received 25 February 2014
Received in revised form 13 June 2014
Accepted 22 June 2014
Available online 7 July 2014

Keywords:
Caveolin–cholesterol interaction
CRAC motif
Phospholipid
Cholesterol distribution
DSC

ABSTRACT

Caveolin-1 is a major structural protein of caveolae and specifically binds cholesterol (Chol). The caveolin scaffolding domain is thought to be involved in caveolin–Chol interaction through the sequence V94-T-K-Y-W-F-Y-R101, a motif that matches a cholesterol recognition amino-acid consensus (CRAC). In the present work, three CRAC-containing peptides, corresponding to caveolin-1 94–101, 82–101 and 93–126, were tested to study the role of the CRAC motif in the caveolin–Chol interaction in 1,2-dipalmitoyl-sn-glycero-3-phosphocholine (DPPC) bilayers using differential scanning calorimetry (DSC), fluorescence and circular dichroism (CD). The Y97I substituents of the three peptides and one peptide segment corresponding to caveolin-1 101–126 that excludes the CRAC motif were also tested for comparison. Our results showed the potency of these CRAC-containing peptides in sequestering Chol into domains and the enhanced role of the intramembrane domain and scaffolding domain for the potency. Of the three CRAC-containing peptides, the peptide 93–126 was particularly effective in promoting Chol segregation, while the peptide 82–101 was less potent in promoting the formation of domains than the peptide 93–126, but was more potent than the peptide 94–101. The domain partition of DPPC/Chol bilayers was not observed in the presence of the peptide 101–126, in contrast to the case in the presence of the peptide 93–126 at the same concentrations of peptide and Chol. The potency of the CRAC motif in Chol segregation was lowered by the Y97I mutation. The difference in structure may be a factor that contributes to different effects of these peptides on the distribution of Chol in the lipid membrane.

1. Introduction

Caveolae are 50–100 nm flask-shaped invaginations of the plasma membranes of most mammalian cells including endothelial cells, macrophages, dendritic cells and adipocytes [1,2]. Caveolins have been identified as integral membrane proteins and an important structural component of caveolae [3]. The caveolin protein family has three members, caveolin-1, -2, and -3 [4]. Caveolin-1 is the prototypical caveolin family member and is therefore the most widely studied of its members. Caveolin-1 is a 22-kDa protein of 178 amino acids and plays a central role in the formation and function of caveolae [5]. Functional studies have shown that caveolin-1 is involved in a wide range of cellular processes, including cell cycle regulation, signal transduction, endocytosis, and cholesterol (Chol) trafficking and efflux [2,6–11]. Although the role of caveolin-1 in regulating signalling molecules is largely unknown, it has been suggested that caveolin-1 may function as a scaffolding protein to organize and concentrate signalling molecules within caveolae [12]. Many signalling molecules, such as epidermal growth factor (EGF) receptor, platelet-derived growth factor (PDGF) receptor, estrogen receptor, H-Ras, and ERK-1/2, have been found to localize in caveolae and interact with caveolin-1 [13–15]. In addition, some enzymes with fundamental vascular functions, such as endothelial nitric oxide synthase (eNOS) and prostacyclin synthase (PGIS), have also been found to be bound to caveolin-1 within caveolae [16–19].

A series of biochemical results have led to a consensus topological model of caveolin-1 although no direct structural information is available [5,20]. Caveolin-1 contains cytoplasmic N- and C-terminal domains that sandwich the membrane-association domains including residues 82–101 (the caveolin scaffolding domain, CSD), residues 102–134 (the intramembrane domain, IMD) and residues 135–150 [17]. The IMD is proposed to form a unique α-helical hairpin that does not completely traverse the membrane [20–22]. Despite inserting into membranes, the IMD was not found to be essential for membrane binding. Rather, two domains adjacent to the IMD, residues 82–101 and 135–150 were found to be largely responsible for high affinity binding to membranes [23–25]. The CSD was suggested to be essential for both caveolin-1 oligomerization and for the interactions of caveolin-1 with other proteins [26]. Associations with other proteins through the CSD may help the coordination of the proteins with receptors and efficient signal

* Corresponding author at: State Key Laboratory of Supramolecular Structure and Materials, Jilin University, 2699 Qianjin Avenue, Changchun 130012, PR China. Tel.: +86 431 85168548; fax: +86 431 85193421.
E-mail address: feili@jlu.edu.cn (F. Li).

http://dx.doi.org/10.1016/j.bbamem.2014.06.018
0005-2736/

transduction [27,28]. However, Collins et al. argued a model of signalling transduction through caveolin–protein interactions at the caveolae in a recent study [29]. Furthermore, mutational studies clearly indicate that CSD is necessary and sufficient for membrane attachment [24]. It has been observed that caveolin-1 truncation mutants that retain the complete N-terminus and the scaffolding domain (caveolin-1 1–101) but lack the intramembrane domain and the palmitoylated C-terminus tightly bind the membrane and target to caveolae. In contrast, caveolin-1 truncation mutants lacking the CSD were found to be completely soluble [25]. Therefore, the CSD seems to be an essential domain for multiple properties of the caveolin-1 molecule. Recent studies on the structures of these caveolin functional segments in various environments including aqueous solutions, micelles and phospholipids confirmed that the IMD relevant segments adopt a helix–break–helix structure and that Pro110 is a key residue for the formation of the helical hairpin structure [30–32], while the CSD relevant segments are β-strand structured [33,34].

Caveolae are enriched with Chol and glycosphingolipids. The binding of caveolin-1 to Chol was found to be tight and specific [35,36]. Caveolin-1 plays an important role in cellular Chol homeostasis, a process that controls intracellular lipid composition and prevents Chol accumulation [37]. It was demonstrated that a dominant-negative caveolin-1 mutant causes intracellular retention of free Chol and a decrease in Chol synthesis as well as efflux of Chol from the cell [38]. Caveolin-1 inserts into membranes of phosphatidylcholine in a Chol-dependent manner [36]. Caveolae are also enriched with saturated fatty acids, mainly palmitic acid C16:0 and stearic acid C18:0, which account for more than 50% of total fatty acids (the other main composition in caveolae is oleic acid) [39–42]. This is quite different from the fatty acid compositions in whole cells. Moreover, palmitic acid and stearic acid are the main fatty acids binding to caveolin-1. However, the acylation or palmitoylation of caveolin-1 is not necessarily required for Chol binding, although it may affect the Chol binding of caveolin-1 [43,44]. When the three palmitoylation sites are mutated, the resulting protein is still translocated to caveolae [45], and the palmitoylation-deficient caveolin-1 mutant is still responsive to Chol-induced stabilization at levels that are virtually identical to those obtained with wild-type caveolin-1 [46]. This suggests that segments of the protein itself facilitate the interaction of caveolin-1 with Chol-rich domains.

The CSD of caveolin-1 contains a consensus sequence -L/V-(X)(1–5)-Y-(X)(1–5)-R/K- in which (X)(1–5) represents one to five residues of any amino acid. The consensus sequence has been found in several proteins that interact with Chol and is referred to as the Chol recognition amino-acid consensus (CRAC) [47,48]. The CRAC motif in CSD corresponds to residues 94–101 with the sequence VTKYWFYR that was suggested to anchor at the membrane interface as an α-helical conformation [49]. Although mutational analysis of the 20-amino-acid CSD domain identified a short membrane attachment sequence KYWFYR that is sufficient to localize a cytoplasmic green fluorescent protein (GFP) to the membrane, the entire CSD is necessary for caveolar membrane targeting [50]. Previous studies using the model membrane 1-stearoyl-2-oleoyl-*sn*-glycero-3-phosphocholine (SOPC) also showed that the KYWFYR sequence does not sequester Chol into domains and has no preferential interaction with Chol, but the CRAC sequence VTKYWFYR does [51,52], further indicating the importance of the CRAC in interactions with Chol.

In order to gain further insight into the role of the CRAC in sequestering Chol into domains, we characterized the interactions of the caveolin-1 intramembrane hydrophobic segment alone (ranging over 101–126) and that flanked by the CRAC motif (ranging over 93–126) with model membrane in this study using differential scanning calorimetry (DSC), fluorescence, and circular dichroism (CD) techniques. We also characterized the interactions of the caveolin-1 CRAC sequence (ranging over 94–101) and CSD segment (ranging over 82–101) with the model membrane and compared the results with those of the intramembrane peptides, by which the roles of the caveolin-1 scaffolding and intramembrane hydrophobic segments in inducing redistribution of Chol in the lipid membrane could be explored. In the CRAC motif sequence of caveolin-1, each of three motif-determining residues V94, Y97, and R101 may play a specific role in the interactions of peptides with Chol. The important role of V94 in interactions of the CRAC motif with Chol was implicated in previous studies that revealed a difference between the KYWFYR and VTKYWFYR sequences in promoting the formation of the Chol domain, as mentioned above [51,52]. In the present study, we focused on another motif-determining residue Y97. The tyrosine side chain has a polar OH group and an aromatic ring that are supposed to facilitate interaction with the interfacial ring component of Chol. Therefore, we substituted the Y97 residue of all the CRAC-containing peptides with a residue with an alkyl side chain, isoleucine (Ile). It is expected that the hydrophobic residue Ile could insert into the membrane more deeply than the polar residue tyrosine, by which the orientation and local structure of the CRAC fragment in the membrane could be changed and thus the interaction of the CRAC segment with Chol could be affected. The lipid 1,2-dipalmitoyl-*sn*-glycero-3-phosphocholine (DPPC) was used as a model membrane in this study for two reasons: 1) saturated fatty acids (16:0 and 18:0) are the main component and main caveolin-1 binding species in caveolae, and DPPC is a saturated lipid with 16 carbon atoms in each hydrocarbon chain; and 2) the mixture of DPPC with even relatively small amount of Chol can result in Chol-rich and Chol-poor domains and these domains display distinct phase transition temperatures in DSC analysis of specific temperature ranges when using water-based solvents, and thus, the redistribution of both Chol and lipids induced by peptides in the membrane mixture can be easily monitored by the change in endotherms.

2. Materials and methods

2.1. Materials

The peptides from human caveolin-1 94–101, 82–101, 93–126 and 101–126, referred to as Cav-1(94–101), Cav-1(82–101), Cav-1(93–126) and Cav-1(101–126), respectively, and the Y97I substituents of the first three peptides, referred to as Cav-1(94–101/Y97I), Cav-1(82–101/Y97I), and Cav-1(93–126/Y97I), were used in this study (Fig. 1). The peptides were synthesized and purified by GL Biochem (Shanghai) Ltd and Shanghai Apeptide Co., Ltd (Shanghai, China). Three lysine (Lys) residues were added on each terminal end of the two 93–126 peptides [Cav-1(93–126) and Cav-1(93–126/Y97I)], while two Lys residues were added in the N-terminus and three Lys residues added in the C-terminus of the Cav-1(101–126) peptide, in order to increase the solubility of the peptides in the purification. Previous studies have demonstrated that tagging hydrophobic peptides with Lys residues does not affect the native characteristics of the peptides inserting in membrane mimetic environments and folding as an α-helical structure, and even oligomeric states ([53] and the references therein). The purity was assessed by high-performance liquid chromatography (HPLC) and mass spectroscopy and was found to be greater than 95%. The phospholipid DPPC was

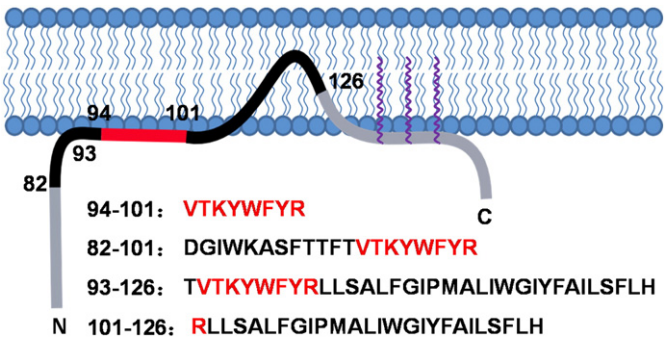

Fig. 1. Schematic representation of the domains of caveolin-1 and the amino acid sequences of the peptide segments of interest in this study.

purchased from Avanti Polar Lipid, Inc. (Alabaster, AL, USA). Chol was obtained from Sigma-Aldrich (St. Louis, MO, USA). The organic solvent 1,1,1,3,3,3-hexafluoro-2-propanol (HFIP, 99.5%) was purchased from Acros Organics (Morris Plains, NJ, USA). All chemicals were used directly after purchase without further purification.

2.2. Sample preparation

Phospholipid DPPC and Chol were separately dissolved in a mixture of chloroform and methanol (2:1 v/v). The peptide powder was dissolved in HFIP solvent to prepare a stock solution. An appropriate volume of peptide stock solution was mixed with the chloroform/methanol co-solvent of DPPC and Chol or DPPC alone. The solvents were then evaporated under a stream of nitrogen to deposit a uniform film of lipid over the bottom of the tube. The obtained lipid film was kept under vacuum overnight to remove residual organic solvents. The dried lipid film was hydrated using 10 mM Na_2HPO_4/NaH_2PO_4 buffer containing 100 mM NaCl at pH 7.4. The lipid film together with the buffer was mixed by vortexing for several seconds. The vesicle suspension was then sonicated using a bath-type sonicator for at least 60 min with caution taken to ensure that the temperature was maintained at 10 °C above the phase transition temperature of the lipids. The small unilamellar lipid vesicles (SUVs) were obtained and used immediately after preparation. The corresponding blank samples without peptides were also prepared using the same methods.

2.3. Fluorescence experiments

Fluorescence measurements were performed using an RF-5301PC spectrofluorophotometer at room temperature. The parameters used for the emission spectra were as follows: scan range, 290–500 nm; excitation, 280 nm; excitation slit, 5 nm; emission slit, 5 nm; and scan rate, medium. Each spectrum was recorded after the average of three scans and the background spectrum was subtracted. For acrylamide quenching experiments, an aliquot of acrylamide from a stock solution of 1 M acrylamide dissolved in buffer was added to the sample solution and the fluorescence spectra were measured. The quenching constant K_{sv} was determined by the Stern–Volmer equation:

$$F_0/F = 1 + K_{sv}[Q] \quad (1)$$

where F_0 and F are the fluorescence intensity in the absence and presence of the quencher (Q), respectively. The samples of 4 μM peptides incorporated with 0.5 mM lipids (P:L 1:125) were used in all fluorescence measurements.

2.4. Differential scanning calorimetry (DSC) measurements

DSC measurements were performed using a Microcal VP-DSC calorimeter (MicroCal, Inc., Northampton, MA, USA) immediately after the preparation of the samples. A 0.5 mL liposome suspension incorporated with peptide was placed in the sample cell and the same volume of buffer was placed in the reference cell. All of the samples were degassed for 10 min at room temperature prior to loading the cell. Samples were heated at a rate of 0. 5 °C/min over a temperature range of 20–60 °C and were equilibrated for 15 min at 20 °C before each scan. Blank experiments with buffer on both cells were also performed for subsequent baseline correction. The expected experimental errors in temperature and enthalpy values were ±0.1 °C and ±5%, respectively. The calorimetric cell was filled with 1.5 mM lipids and 18.75 μM peptides (peptide-to-lipid mole ratio P:L = 1:80). The concentrations of 100 μM were also used for Cav-1(94–101) and Cav-1(94–101/Y97I) (P:L = 1:15). The Chol composition was varied from 0 to 20% in mole fraction.

Buffer subtraction and baseline correction were performed using Microcal Origin software (MicroCal, Northampton, MA, USA). The DSC profiles were analysed by decomposition of the main transition peaks into two individual components with Lorenz lineshape and fitted as the sum of the components using the non-linear least square curve fitting procedure supplied with the Origin 8.0 software.

2.5. Circular dichroism (CD) measurements

The CD spectra were recorded on a PMS-450 spectropolarimeter (Biologic, France) at room temperature using a 0.5-mm path-length quartz. Samples of 24 μM peptides and 3 mM lipids (P:L 1:125) were used. Data were recorded from 190 to 260 nm at a speed of 0.1 nm/s. The background signal was subtracted from all spectra. The intensities of the final spectra were expressed as mean residue ellipticity. The secondary structure contents were estimated by the CDPro software package using the program CONTIN/LL. A reference set of SMP56 including 56 proteins was used in the analyses of CD data.

3. Results

3.1. Thermotropic phase behaviors of DPPC vesicles in the presence of Chol

The heating scan of pure DPPC showed two endothermic transitions (Fig. 2). The broad one centred at 34.5 °C corresponds to the pre-transition from a lamellar gel phase ($L_{\beta'}$) to a rippled gel phase ($P_{\beta'}$), and the sharp one at 41.6 °C corresponds to the main transition from the rippled gel phase to the liquid crystal phase (L_α) [54,55]. Upon incorporation of 15 mol% and 20 mol% Chol into the DPPC vesicles, the pre-transition peaks were broadened or abolished and the main transition peaks display an obviously asymmetric broadening (Fig. 2). We deconvolved the heat capacity profiles of the main transition peaks in the presence of Chol into two components and obtained a sharper peak that has a transition temperature lower than that of pure DPPC and a broader peak that has a transition temperature higher than that of pure DPPC. The parameters including the transition temperature, cooperativity and melting enthalpy of each component (represented by $T_{m(1)}$, $\Delta T_{1/2(1)}$, and ΔH_1 for the transition at lower transition temperature, and $T_{m(2)}$, $\Delta T_{1/2(2)}$, and ΔH_2 for the transition with higher transition temperature, respectively), and the total endothermic melting

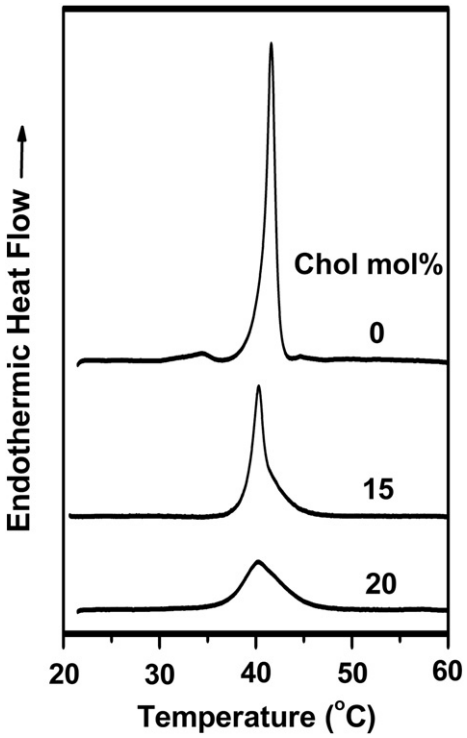

Fig. 2. DSC thermograms of DPPC alone and DPPC with 15 mol% and 20 mol% Chol.

enthalpy of the transition (ΔH_t), were obtained using two-component fitting of the DSC endotherms (Table 1 and Fig. S1 in Supplementary Materials). The component at $T_{m(1)}$ is attributed to the Chol-poor domain and the other component at $T_{m(2)}$ is attributed to the Chol-rich domain [56].

The addition of more quantities of Chol generated more perturbation to the Chol-poor domain than to the Chol-rich domain, which amplified the difference in the packing of lipid chains between the two domains and, thus, caused a larger ΔT_m. Moreover, a slightly larger percentage of ΔH_2 in ΔH_t ($P_{\Delta H2}$ in Table 1) for 20 mol% Chol also suggests somewhat more perturbation of Chol to the Chol-poor domain than to the Chol-rich domain.

Considering that the pre-transition peaks were not observed in the presence of Chol, we focused only on the thermotropic phase behaviors of the main transition peaks in the following sections.

3.2. Thermotropic phase behaviors of DPPC vesicles mixed with peptides 94–101 and Chol

The incorporation of peptides Cav-1(94–101) and Cav-1(94–101/Y97I) with DPPC vesicles gave rise to a small decrease in the main transition temperature T_m and a broadening of the peak width $\Delta T_{1/2}$ (or a decrease in cooperativity) along with the broadening or vanishing of the pre-transition peak. The endothermic melting enthalpy of the DPPC vesicles was slightly affected by the two peptides (Fig. 3 and Table 2). The addition of both 15 mol% and 20 mol% Chol in the peptide-containing DPPC lipids at P:L of 1:80 resulted in a dramatic decrease both in cooperativity and enthalpy and a decrease in T_m of the endothermic transition. When the ratio of P:L was increased to 1:15, a distinct separation of the main transition peaks was observed and the peak separation increased from 15 mol% Chol to 20 mol% Chol. Similar to the results for peptide-free vesicles, a sharper peak at the lower transition temperature corresponding to the Chol-poor domain and a broader peak at the higher transition temperature corresponding to the Chol-rich domain were obtained by the two-component fitting of the thermograms of the DPPC/peptide/Chol mixed vesicles (Fig. S2 in Supplementary Materials), and the thermotropic phase data of the two components are listed in Table 2. In the presence of peptides, the ΔH_t of the DPPC vesicles also decreased with increasing mole faction of Chol, which is consistent with the effect of Chol on pure DPPC vesicles.

Despite similar thermotropic phase behavior, the liposomes with the wild-type peptide and its Y97I mutant displayed small but distinct differences in ΔT_m and $P_{\Delta H2}$ of the phase transition, suggesting the difference of the two peptides in inducing distribution of Chol in DPPC bilayers. The $P_{\Delta H2}$, instead of ΔH_2, was used to compare the difference between the perturbations of Chol to lipid chains in the Chol-rich domain of DPPC bilayers with the wild-type peptide and Y97I mutant considering the different effects of the two peptides on the enthalpy of the pure DPPC membrane. Interestingly, the $P_{\Delta H2}$ values of DPPC vesicles in the presence of Cav-1(94–101) were smaller than those in the presence of Cav-1(94–101/Y97I) at P:L 1:15, meaning that the phase transition of the Chol-rich domain in the presence of the wild-type peptide requires smaller fraction of enthalpy than it does in the presence of the Y97I mutant. This suggests that the packing of lipids in the Chol-rich domain may be disturbed to a larger extent in the presence of the wild-type peptide than in the presence of the mutant. It is likely that the lipids were present in the Chol-rich domain in a smaller quantity in the presence of the wild-type peptide than in the presence of the mutant. In addition, ΔT_m induced by the wild-type peptide was larger than that induced by the mutant at 20 mol% Chol, further confirming that the larger difference in lipid packing between the Chol-rich and the Chol-poor domains was induced by the wild-type peptide than the mutant.

3.3. Thermotropic phase behaviors of DPPC vesicles mixed with peptides 82–101 and Chol

The DSC thermograms of DPPC vesicles incorporated with two 82–101 peptides at P:L 1:80 displayed a single main transition peak with a broader $\Delta T_{1/2}$ and lower T_m than those of pure DPPC. The melting enthalpies of the main transitions were also lowered in the presence of the peptides. The addition of 15 mol% Chol in the peptide-containing DPPC vesicles further induced a decrease in cooperativity, T_m and ΔH_t of the main transition, but not peak separation. The peak separation was observed in the DSC endotherms of the peptide-containing DPPC vesicles only when the amount of Chol was increased to 20 mol% (Fig. 4). Decomposition of the heat capacity profiles by two components gave rise to a sharper peak at a lower T_m (Chol-poor domain) and a broader peak at a higher T_m (Chol-rich domain), as shown in Fig. S3 in the Supplementary Materials. A larger separation between the two transition components (larger ΔT_m) and a smaller percentage of enthalpy (smaller $P_{\Delta H2}$) from the Chol-rich domain in the presence of Cav-1(82–101) than in the presence of Cav-1(82–101/Y97I) were obtained by fitting of the DSC endotherm profiles of the DPPC/peptide/Chol vesicles (Table 3).

3.4. Thermotropic phase behaviors of DPPC vesicles mixed with peptides 93–126 and Chol

The DSC thermograms of DPPC vesicles containing two peptides 93–126 also displayed a single main transition peak with a decreasing T_m and an increasing $\Delta T_{1/2}$ with respect to pure DPPC. The ΔH_t of the transition decreased in the presence of the Y97I mutant, while it slightly changed in the presence of the wild-type peptide. With the addition of both 15 mol% and 20 mol% Chol, an evident partition of the domain was observed in the DSC thermograms of the peptide-containing DPPC vesicles, and the partition was more pronounced with the increase in Chol from 15 mol% to 20 mol% (Fig. 5). Decomposition of the DSC endotherms demonstrated a general pattern of two peaks with $\Delta T_{1/2(1)}$ smaller than $\Delta T_{1/2(2)}$ for the mixture of DPPC with peptides in the presence of Chol except for the DPPC vesicles mixed with Cav-1(93–126) and 15 mol% Chol which displayed the DSC endotherm of two peak components with $\Delta T_{1/2(1)}$ slightly larger than $\Delta T_{1/2(2)}$ (Fig. S4 in Supplementary Materials). Although the two peptides exerted similar effects on the endothermic behaviors of the DPPC/Chol bilayers, differences in $P_{\Delta H2}$ and ΔT_m, were still present, i.e., the ΔT_m values in the presence of the mutant were smaller than those in the

Table 1
The phase transition data of DPPC vesicles with varying mole fractions of Chol.

Chol mol%	$T_{m(1)}$ °C	$\Delta T_{1/2(1)}$ °C	ΔH_1 kcal/mol	$T_{m(2)}$ °C	$\Delta T_{1/2(2)}$ °C	ΔH_2 kcal/mol	ΔH_t kcal/mol	ΔT_m °C	$P_{\Delta H2}$%
0[a]	41.6	1.1	6.1				6.1		
15	40.3	1.4	3.2	42.2	2.3	1.0	4.2	1.9	24
20	40.1	3.3	2.5	42.3	3.4	0.9	3.4	2.2	27

[a] The main phase transition of pure DPPC in DSC endotherm is a single peak. Thus $T_{m(1)}$, $\Delta T_{1/2(1)}$ and ΔH_1 of pure DPPC represent the T_m, $\Delta T_{1/2}$ and ΔH_t of the single transition, but not those of the peak component at lower transition temperature. We list them like this just for simplicity. The same expression is also used in Tables 2–4.

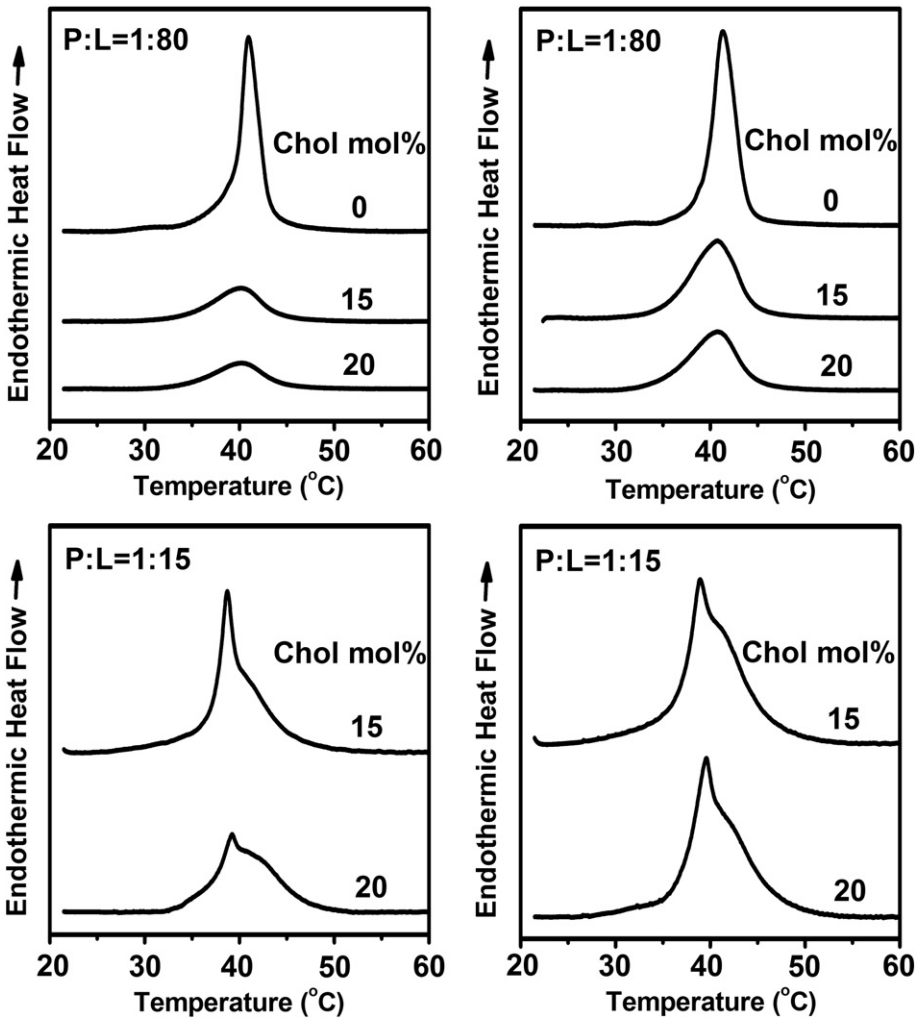

Fig. 3. DSC thermograms of DPPC vesicles incorporated with the peptides 94–101 (left: wild-type peptide; right: mutant) and various quantities of Chol.

presence of the wild-type peptide and the $P_{\Delta H2}$ values induced by the mutant were larger than those induced by the wild-type peptide (Table 4).

3.5. The thermotropic phase behaviors of DPPC vesicles mixed with Cav-1(101–126) and Chol

In contrast to the thermotropic behaviors of DPPC vesicles mixed with Chol and the CRAC-containing peptide Cav-1(93–126), no observable separation of transition peak was detected in the DSC endotherms of the DPPC vesicles mixed with Chol and the CRAC-removed peptide Cav-1(101–126) at P:L 1:80, but a single transition peak with an evidently broadening line width and a decreasing transition temperature appeared. The melting transition enthalpies of the lipid mixtures in the presence of both 15 mol% and 20 mol% Chol were much smaller than those were in the absence of Chol (Fig. 6 and Table 5). The perturbation of the peptide to DPPC vesicles in the absence of Chol caused an increase in both ΔH_t and $\Delta T_{1/2}$ and a decrease in T_m with respect to pure DPPC.

Table 2
The phase transition data of DPPC vesicles with varying mole fractions of Chol in the presence of peptides 94–101.

P:L	Chol mol%	Peptide	$T_{m(1)}$ °C	$\Delta T_{1/2(1)}$ °C	ΔH_1 kcal/mol	$T_{m(2)}$ °C	$\Delta T_{1/2(2)}$ °C	ΔH_2 kcal/mol	ΔH_t kcal/mol	ΔT_m °C	$P_{\Delta H2}$%
1:80	0[a]	Wildtype	41.0	2.0	6.3				6.3		
		Mutant	41.3	2.7	6.4				6.4		
	15[a]	Wildtype	40.1	5.9	3.6				3.6		
		Mutant	40.7	5.5	4.8				4.8		
	20[a]	Wildtype	40.3	6.1	2.9				2.9		
		Mutant	40.8	5.8	3.8				3.8		
1:15	0[a]	Wildtype	40.7	1.9	6.4				6.4		
		Mutant	41.0	1.7	8.5				8.5		
	15	Wildtype	38.7	1.3	1.8	40.3	6.3	4.1	5.9	1.6	69
		Mutant	38.8	1.6	1.3	40.7	6.6	4.1	5.4	1.9	76
	20	Wildtype	39.2	3.5	2.0	42.4	5.0	1.9	3.9	3.2	49
		Mutant	39.4	2.6	1.9	42.1	6.1	2.6	4.5	2.7	58

[a] See the note in Table 1.

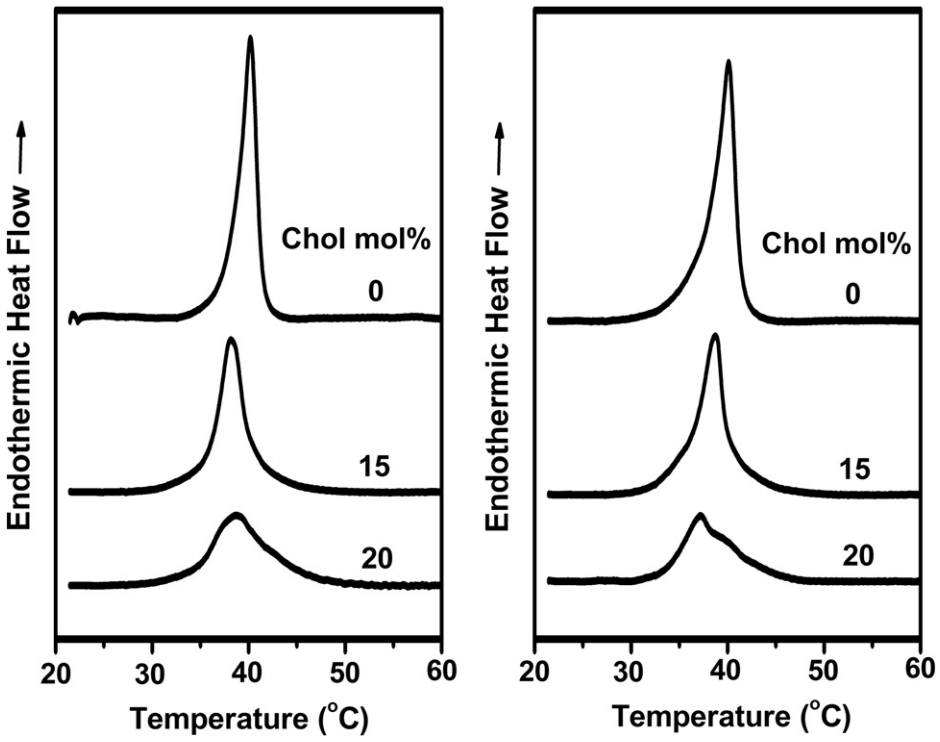

Fig. 4. DSC thermograms of DPPC vesicles incorporated with the peptides 82–101 (left: wild-type peptide; right: mutant) and various quantities of Chol.

3.6. Fluorescence of the peptides incorporated with the DPPC/Chol vesicles

The fluorescence spectra of the peptides incorporated with the DPPC lipids including 50 mol% Chol and those of Chol-free vesicles are shown in Fig. 7. The emission maxima were mostly unchanged following the addition of Chol, remaining fixed at ~342 nm and ~350 nm for Cav-1(94–101) and Cav-1(94–101/Y97I), respectively, ~342–344 nm for two 82–101 peptides, ~334 nm for two 93–126 peptides and ~339 nm for Cav-1(101–126). Previous studies have shown that the fluorescence emission at ~330 nm is related to a hydrophobic ambient of tryptophan (Trp), while the fluorescence emission at ~350 nm is related to the exposure of the chromophore to a polar ambient [57]. Accordingly, the Trp residues of the intramembrane peptides could be inserted in the membrane more deeply than the 82–101 and 94–101 peptides either in the absence or in the presence of Chol. The mixture of 50 mol% Chol with DPPC lipids resulted in a reduction in fluorescence intensity of the six CRAC-containing peptides. However, the magnitude of the Chol-induced intensity reduction in the presence of the wild-type peptides was different from that in the presence of the mutants. As shown in Fig. 7, the fluorescence intensities of the wild-type peptides were higher than those of the mutant peptides in the absence of Chol, while the intensities of the former were lower than [for Cav-1(94–101) and Cav-1(82–101)] or close to [for Cav-1(93–126)] those of the latter in the presence of Chol. The wild-type peptides displayed greater decrease in the intensity than did the mutants. It is noted that there are two Trp residues on two 93–126 peptides, but only one fluorescence peak was observed, indicating that the two Trp residues were involved in the same or very similar environment. The addition of 50 mol% Chol in the DPPC vesicles with Cav-1(101–126) also caused a decrease in fluorescence intensity of the peptide. However, the magnitude of the decrease in intensity was much smaller than those of two 93–126 peptides.

The effect of Chol on the position of the peptides in the membrane was further characterized by the acrylamide quenching experiments and the quenching constant K_{sv} that is associated with accessibility of the quencher to Trp was obtained. As shown in Fig. 8 (also see Figs. S5–S9 in Supplementary Materials), the K_{sv} values of the wild-type peptides were smaller than those of the Y97I mutants were in the absence of Chol, but contrasting results were obtained in the presence of Chol for all CRAC-containing peptides. Moreover, the K_{sv} values of all peptides, either the wild-type peptides or the Y97I mutants, were larger in the presence of Chol than those were in the absence of Chol and the Chol-induced changes in K_{sv} were larger in the presence of the wild-type peptides than in the presence of the mutants.

3.7. Secondary structures of the peptides incorporated with the DPPC/Chol vesicles

The secondary structures of the peptides incorporated with the DPPC vesicles were monitored by Far-UV CD spectra in the absence and

Table 3
The phase transition data of DPPC vesicles with varying mole fractions of Chol in the presence of peptides 82–101 at P:L 1:80.

Chol mol%	Peptide	$T_{m(1)}$ °C	$\Delta T_{1/2(1)}$ °C	ΔH_1 kcal/mol	$T_{m(2)}$ °C	$\Delta T_{1/2(2)}$ °C	ΔH_2 kcal/mol	ΔH_t kcal/mol	ΔT_m °C	$P_{\Delta H2}$%
0[a]	Wildtype	40.2	1.9	5.3				5.3		
	Mutant	40.1	2.4	5.9				5.9		
15[a]	Wildtype	38.1	2.8	4.8				4.8		
	Mutant	38.7	2.8	4.7				4.7		
20	Wildtype	38.4	4.7	2.9	42.0	5.6	1.0	3.9	3.6	26
	Mutant	36.9	3.2	1.7	40.0	5.0	1.3	3.0	3.1	44

[a] See the note in Table 1.

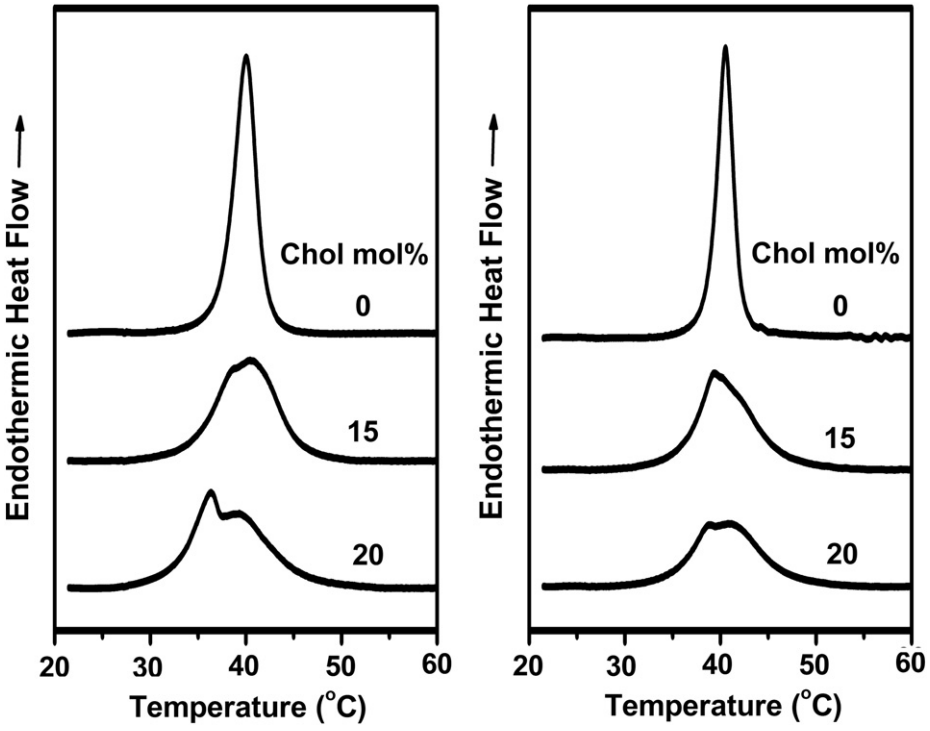

Fig. 5. DSC thermograms of DPPC vesicles incorporated with the peptides 93–126 (left: wild-type peptide; right: mutant) and various quantities of Chol.

presence of Chol (Fig. 9). In the absence of Chol, the CD spectra demonstrated a characteristic of disordered structure for two 94–101 peptides, a substantial β-sheet structure for two 82–101 peptides and an α-helical structure for two 93–126 peptides and the 101–126 peptide. With the addition of 50 mol% Chol, a weak positive absorbance at ~ 231 nm appeard for two 94–101 peptides. These absorbances may be associated with the contribution of Trp98 [58]. The CD curves demonstrated a slight decrease in the negative absorbance at ~ 218 nm for Cav-1(82–101), but a slight increase in this absorbance for Cav-1(82–101/Y97I), in the presence of 50 mol% Chol. The presence of Chol also resulted in a slight decrease in the negative absorbances at ~ 210 nm and 222 nm for the peptides 93–126. An obvious decrease in the intensity of the negative absorbance was detected for Cav-1(101–126) with the addition of Chol. The secondary structure contents of two scaffold peptides and three intramembrane peptides in DPPC alone and in DPPC vesicles containing 50 mol% Chol were calculated based on the deconvolution of the CD spectra and the results are listed in Table 6.

The secondary structures of the 93–126, 101–126 and 82–101 peptides incorporated with the DPPC lipids were further estimated by the attenuated total reflection Fourier transform infrared (ATR-FTIR) spectra. The polarization-independent spectra that was obtained from combination of the parallel and perpendicular polarized spectra of the amide I region (1600–1700 cm^{-1}) were analysed using curve fitting method and the secondary structure contents of the peptides in the membrane were represented by the percentage of the area of the specific secondary structure bands in the total band area. The experimental details, the ATR-FTIR spectra, the band assignments and the secondary structure contents of the peptides are shown in the Supplementary Materials (Figs. S10–S12, Tables S1 and S2). The typical absorbance regions of the different secondary structure components were assigned as follows: α-helix 1651–1657 cm^{-1}, β-sheet 1609–1636 cm^{-1} and 1684–1695 cm^{-1}, β-turn 1662–1678 cm^{-1}, and random 1637–1646 cm^{-1} [59]. To avoid the perturbation of H_2O absorbance, the lipid membranes used in the ATR-FTIR experiments were hydrated by D_2O, instead of the phosphate buffer that was used in CD experiments. In addition, the peptides were associated with flat multi-layer membranes in the ATR-FTIR experiments, while the peptides were incorporated with SUVs in the CD experiments. The differences in experimental conditions could have certain effects on the data of the secondary structures, nevertheless, the results obtained by the two methods were comparable (See Tables 6 and S2 in Supplementary Materials).

4. Discussion

Caveolin-1 is a Chol-binding protein with an approximate 1:1 stoichiometry in the presence of 0.2% sodium dodecyl sulfate (SDS). Binding of caveolin-1 to Chol is critical for maintenance of the caveolar structure and protein function [3]. The segment consisting of the residues 94–101 with the VTKYWFYR sequence in the amino-terminal region of caveolin-1 has been suggested to be a Chol recognition domain of the

Table 4
The phase transition data of DPPC vesicles with varying mole fractions of Chol in the presence of peptides 93–126 at P:L 1:80.

Chol mol%	Peptide	$T_{m(1)}$ °C	$\Delta T_{1/2(1)}$ °C	ΔH_1 kcal/mol	$T_{m(2)}$ °C	$\Delta T_{1/2(2)}$ °C	ΔH_2 kcal/mol	ΔH_t kcal/mol	ΔT_m °C	$P_{\Delta H2}$%
0[a]	Wildtype	40.0	2.7	6.4				6.4		
	Mutant	40.4	2.0	5.0				5.0		
15	Wildtype	38.6	4.8	3.0	41.6	4.2	2.7	5.7	3.0	44
	Mutant	39.3	3.7	2.4	42.0	5.4	2.3	4.7	2.7	50
20	Wildtype	35.9	3.4	2.3	39.9	6.5	3.4	5.7	4.0	60
	Mutant	38.5	3.5	1.2	41.7	6.0	2.7	3.9	3.2	69

[a] See the note in Table 1.

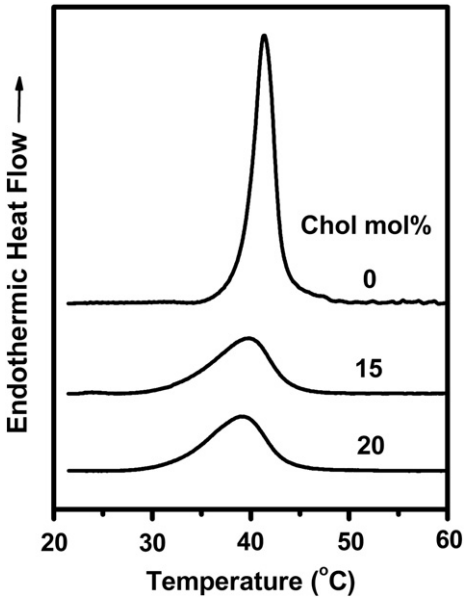

Fig. 6. DSC thermograms of DPPC vesicles incorporated with the peptides 101–126 and various quantities of Chol.

protein. This CRAC motif belongs to a part of the CSD domain and flanks the hydrophobic segment comprising residues 105–125 that is suggested to play a role in anchoring caveolin-1 to the membrane [22]. In this study, we aimed to explore the role of the CRAC in sequestering Chol into a domain and to evaluate the effects of the caveolin-1 scaffolding and intramembrane hydrophobic segments on the CRAC activity in Chol segregation. Thus, we selected in this study three CRAC-containing peptides including residues 94–101 (CRAC motif), 82–101 (CSD segment), and 93–126 (CRAC-flanked intramembrane hydrophobic segment) and the peptide 101–126 (intramembrane hydrophobic segment without CRAC). We obtained corresponding information by analysing both the peptide-induced changes in the thermotropic phase behaviors of the lipid membrane with Chol and the Chol-induced changes in the environment and structure of the peptides in the lipid membrane observed by DSC, fluorescence and CD experiments, respectively.

The DSC studies demonstrated that Chol is not miscible with the DPPC lipid membrane at 15% and 20% mole fraction and the non-miscibility leads to the compartmentalization of the membrane into two domains, namely a Chol-rich domain and a Chol-poor domain. Incorporation of all the caveolin-1 peptides studied here results in a redistribution of Chol in the DPPC membrane. However, the redistribution of Chol in the DPPC membrane was different in the presence of different peptides. In particular, the peptide that contains the CRAC motif displayed a distinct difference in its affect on the distribution of Chol in the membrane from the peptide that does not contain the CRAC motif, as demonstrated by the DSC results of the DPPC/Chol bilayers in the presence of Cav-1(93–126) and Cav-1(101–126). The formation of domains was facilitated by the peptide Cav-1(93–126) in the DPPC membrane with both 15 mol% and 20 mol% Chol, whereas a dispersive distribution of Chol instead of clustering of Chol in the lipid membrane was mediated by Cav-1(101–126). The presence of Cav-1(101–126) in the DPPC membrane was unfavorable for Chol segregation, likely due to the non-specific interaction of the peptide with Chol. In contrast, there is a specific interaction of the CRAC-containing peptide with Chol, which results in the formation of a Chol-rich domain [60]. The difference between the two peptides in regulating distribution of Chol in the DPPC membrane suggests the important role of the CRAC motif in sequestering Chol into domains.

Table 5
The phase transition data of DPPC vesicles with varying mole fractions of Chol in the presence of Cav-1(101–126) at P:L 1:80.

Chol mol%	T_m °C	$\Delta T_{1/2}$ °C	ΔH_t kcal/mol
0	41.4	2.4	6.6
15	39.9	6.7	3.2
20	39.0	6.7	3.2

The difference of the peptides in regulating Chol distribution in the DPPC membrane was also observed in studies of other CRAC-containing caveolin-1 peptides. Compared with Cav-1(93–126), the peptide Cav-1(82–101) mediates the membrane partitioning only at a higher Chol mole fraction (20 mol%) with a smaller ΔT_m. At a lower mole fraction of Chol (15 mol%), the membrane partitioning was not generated by the addition of Cav-1(82–101) in the DPPC lipids. For the short peptide Cav-1(94–101), the separation of domains was not observed in the DPPC membrane with both 15 mol% and 20 mol% Chol at the same P:L ratio (1:80). Only when the P:L ratio was increased to 1:15 the membrane partitioning was mediated by the peptide Cav(94–101). This suggests that the shorter peptides Cav-1(82–101) and Cav-1(94–101) have a weaker interaction with Chol than the intramembrane peptide Cav-1(93–126). In consequence, either greater quantity of peptide molecules or greater quantity of Chol molecules is needed for sequestering Chol into domains. Compared with the peptide Cav-1(94–101), the CSD peptide Cav-1(82–101) was more potent in mediating tight packing of Chol in the lipid membrane. The differences among the peptides in mediating Chol segregation reveal that the intramembrane hydrophobic segment plays an important role in facilitating the interaction of the CRAC motif with Chol. The segment in the N-terminal part of the scaffold peptide was also considerably helpful for targeting of the CRAC motif to Chol, as indicated by the results showing that the longer peptide Cav-1(82–101) was more potent in sequestering Chol, albeit less effective than the intramembrane hydrophobic segment, compared with the shorter peptide Cav-1(94–101) in the lipid membrane containing 20 mol% Chol at P:L 1:80. Similar results were also obtained by R. M. Epand et al. in their study of the peptide Cav-1(83–102) and Cav-1(94–101) in a mixture of SOPC and Chol [52]. Apparently, the efficiency of the CRAC motif in Chol segregation was augmented by the extension of the sequence to either the N-terminal part of the CSD or the intramembrane domain. Evaluation of the secondary structure via CD and ATR-FTIR experiments demonstrated that the peptides Cav-1(94–101), Cav-1(82–101) and Cav-1(93–126) adopt predominantly random, β-sheet and α-helix conformations, respectively. Different conformations of the three peptides in the membrane may be a factor contributing to their different effects on the distribution of Chol in the lipid membrane. It was suggested that a smooth, uniform surface contour of a transmembrane helix would more readily mix with a rigid Chol-rich domain [61]. Although the IMD segment of Cav-1 is proposed to form a helix–break–helix structure [30–32], the interaction of the IMD with Chol by the helical fragments in the hairpin structure may still be favorable for targeting of the Cav-1 protein to the Chol-rich domain.

In general, three aspects should be considered for the effects of a peptide on the distribution of Chol in the DPPC membrane. The first is more favorable interaction of the peptide with Chol than with DPPC lipids, the second is avoidance of the peptide from interacting with Chol, and the third is that the peptide neither specifically favors nor avoids Chol. Either the first or the second factor facilitates the formation of a Chol-rich domain [60]. In contrast, the third factor may increase miscibility of Chol with lipids. The thermotropic phase behavior of DPPC/Chol bilayers in the presence of Cav-1(101–126) shows a predominant role of the third factor in the distribution of Chol in the lipid membrane, which leads to an approximately homogeneous distribution of Chol in the bilayers and fusion of domains. However, the thermotropic phase behaviors of the DPPC/Chol bilayers in the presence of the CRAC-containing peptides show a predominant role of the first factor in the distribution of Chol in the lipid membrane, and, thus, the segregation of bilayers was promoted. Compared with the lipid distribution in

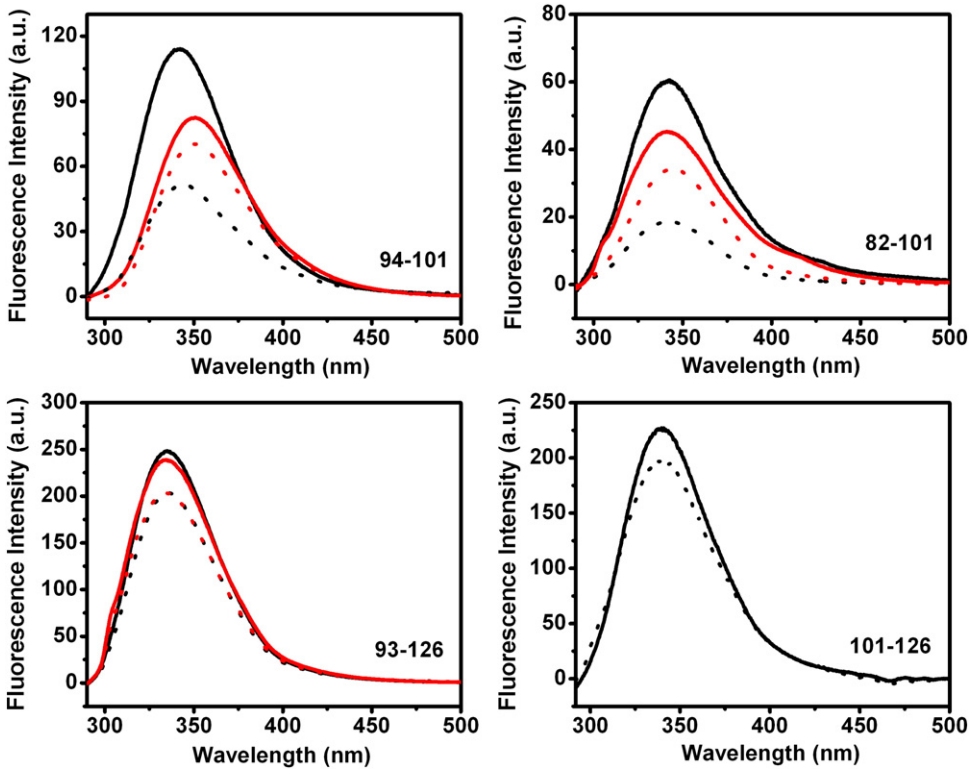

Fig. 7. Fluorescence spectra of the caveolin-1 peptides (black: wild-type peptides, red: mutants) incorporated with DPPC alone (solid line) or DPPC containing 50 mol% Chol (dot line).

the peptide-free membrane, more lipids may be involved in the Chol-rich domain in the presence of the CRAC-containing peptide. The involvement of more lipids in the Chol-rich domain makes Chol molecules in this domain less tightly packed than they do in the peptide-free membrane, which could cause the increase in ΔH_2 with respect to the peptide-free bilayers.

The role of Tyr at position 97 of caveolin-1 in the interaction of the CRAC-containing peptides with Chol was characterized by monitoring the thermotropic phase behaviors of the DPPC bilayers mixed with Chol and Y97I mutants. Compared with the wild-type peptides, the presence of the mutants does not cause an intrinsic change in the thermotropic phase behaviors of the DPPC/Chol membranes, but only results in a small increase in $P_{\Delta H2}$ and decrease in ΔT_m if separation of endothermic peaks occurs in the DSC thermographs. The fact that the potency of the peptides in sequestering Chol into domains is only reduced and not abolished by the substitution of Ile to Tyr suggests that the Tyr at position 97 plays a role in the interaction of caveolin-1 with Chol, but other residue(s) in the CRAC motif may also play a role in the specific interaction of the protein with Chol [50]. Nevertheless, a slightly larger $P_{\Delta H2}$ and smaller ΔT_m in the presence of the mutant peptides than in the presence of the wild-type peptides indicate that the Chol-rich domain of the DPPC lipid membrane was less tightly packed in the presence of the mutants than in the presence of the wild-type peptides likely due to involvement of more lipids in the Chol-rich domain in the presence of the mutants.

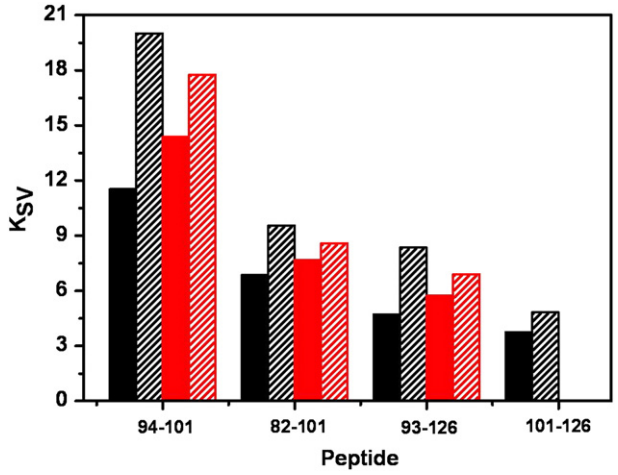

Fig. 8. K_{sv} data obtained by acrylamide quenching to Trp residues of the caveolin-1 peptides (black: wild-type peptides, red: mutants) incorporated with DPPC alone (fully filled) or DPPC containing 50 mol% Chol (filled with dense line).

The fluorescence emission spectra of the Trp residues in the peptides were used to monitor the distribution of the peptides in the DPPC lipid vesicles containing 50% mole fraction of Chol. The DPPC bilayers with 50 mol% Chol are characterized by a liquid-ordered (L_o) phase [62,63], in which hydrocarbon chains of lipids are extended and ordered as in the gel phase, but the lateral mobility in the bilayer is very high as in the disordered (I_d) phase [64]. The L_o phase is proposed to be more representative of the membrane organization of caveolae and rafts [65]. Our results show that the addition of Chol in DPPC vesicles leads to a decrease in fluorescence intensity and an increase in K_{sv} for all the peptides studied. This suggests that the presence of Chol induces a movement of the peptides in the DPPC lipid membrane from a deeper position in the absence of Chol to a more solvent exposed position. Interestingly, the peptide Cav-1(101–126) that has no CRAC motif shows a lower magnitude of change either in fluorescence intensity or in K_{sv} from the Chol-containing membrane to the Chol-free membrane than the peptide Cav-1(93–126) that contains the CRAC motif, suggesting that Cav-1(93–126) populates the Chol-rich domain with more quantity than Cav-1(101–126) and further confirming that the CRAC motif was critical in the interaction of caveolin-1 peptide segments with Chol. For the CRAC-containing peptides, either the decrease in fluorescence intensity or the increase in the acrylamide quenching

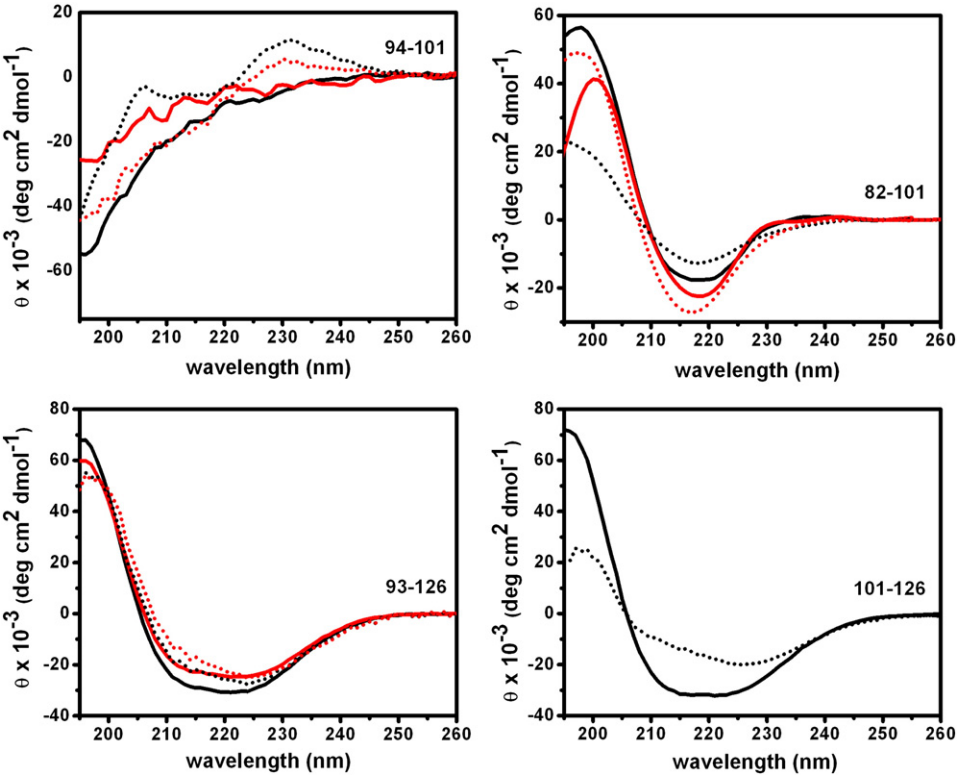

Fig. 9. CD spectra of the caveolin-1 peptides (black: wild-type peptides, red: mutants) incorporated with DPPC alone (solid line) or DPPC containing 50 mol% Chol (dot line).

constant induced by Chol was more pronounced for the wild-type peptides than those for the mutants, suggesting that the Trp residues of the wild-type peptides undergo a more significant change in environments from the Chol-free membrane to the Chol-containing membrane than those of the mutants, possibly through more preferential interaction of the wild-type peptides with Chol than the mutants.

The effects of Chol on the secondary structures of the peptides in DPPC bilayers were also probed by CD and ATR-FTIR measurements. Although there were some differences in the values from the two methods possibly due to the differences in the experimental conditions and spectral treatment methods, comparable conclusions could be drawn from the two sets of the secondary structure data. In general, three intramembrane peptides form an α-helical structure. The presence of Chol resulted in an evident decrease in helicity for Cav-1(101–126), while the Chol-induced change in helicity of Cav-1(93–126) was rather small, indicating a role of the CRAC motif in the interaction with Chol. It seems that the interaction of the CRAC motif with Chol has an effect of stabilizing helical folding of the IMD peptide in the ordered lipid membrane. The Y97I mutation in the CRAC motif results in a decrease in α-helix folding, which likely occurrs in the CRAC region, both in the absence and presence of Chol, suggesting that the Y97I mutation destabilizes the helical structure. Unlike the intramembrane peptides, the peptide Cav-1(82–101) predominantly adopts a β-sheet structure and a small amount of helical structure in the pure DPPC membrane. The helix structure was transferred to the β-strand (CD result) or β-turn (ATR-FTIR result) by the Y97I mutation, further suggesting a destabilizing effect of the Y97I mutation on helical structure and the short helical structure may be formed in the CRAC region. The addition of Chol results in a decrease in the α-helix content for the wild-type peptide and an increase in the β-strand content for the mutant. This suggests that the presence of Chol in the DPPC membrane is unfavorable to the α-helix structure, but is favorable to the β-sheet structure for the scaffolding peptides 82–101. The two 94–101 peptides were unstructured in the lipid membrane either with or without Chol. It seems that the formation of the helical structure in the CRAC region of a wild-type peptide is associated with peptide length and insertion of the peptide in the membrane.

Table 6
Secondary structure data for the caveolin-1 peptides in pure DPPC and DPPC vesicles with 50 mol% Chol obtained by the CD measurements.

Peptide	Chol (mol%)	Secondary structure (%)			
		Helix	Strand	Turn	Unordered
Cav-1(82–101)	0	20	61	4	15
	50	5	61	17	17
Cav-1(82–101/Y97I)	0	0	77	8	15
	50	9	85	0	6
Cav-1(93–126)	0	77	8	8	7
	50	75	10	9	6
Cav-1(93–126/Y97I)	0	69	16	6	9
	50	69	7	14	10
Cav-1(101–126)	0	76	9	9	6
	50	61	3	36	0

5. Conclusions

All the CRAC-containing peptides from caveolin-1 in this study displayed the potential to interact with Chol in the DPPC lipid membrane. The preferential interactions of the CRAC-containing peptides with Chol could facilitate Chol segregation in the DPPC membrane, which depends on peptide properties or Chol concentration. The potency of the CRAC motif in Chol segregation was either significantly enhanced by the linking with the IMD segment that was inserted into membrane inner or was enhanced to a less extent by linking of the residues in the CSD N-terminal part which may attach to the membrane surface. The potency of the CRAC-containing peptides in Chol segregation was lowered by the Y97I mutation and was completely lost by the deletion of the CRAC motif. Different conformations of the peptides could be a factor that contributes to their different effects on the distribution of Chol in the lipid membrane.

Acknowledgement

This work was financially supported by the NSFC (20934002).

Appendix A. Supplementary data

Supplementary data to this article can be found online at http://dx.doi.org/10.1016/j.bbamem.2014.06.018.

References

[1] J. Harris, D. Werling, J.C. Hope, G. Taylor, C.J. Howard, Caveolae and caveolin in immune cells: distribution and functions, Trends Immunol. 23 (2002) 158–164.
[2] F. Galbiati, D. Volonte, J. Liu, F. Capozza, P.G. Frank, L. Zhu, R.G. Pestell, M.P. Lisanti, Caveolin-1 expression negatively regulates cell cycle progression by inducing G(0)/G(1) arrest via a p53/p21(WAF1/Cip1)-dependent mechanism, Mol. Biol. Cell 12 (2001) 2229–2244.
[3] K.G. Rothberg, J.E. Heuser, W.C. Donzell, Y.S. Ying, J.R. Glenney, R.G. Anderson, Caveolin, a protein component of caveolae membrane coats, Cell 68 (1992) 673–682.
[4] T.M. Williams, M.P. Lisanti, The caveolin proteins, Genome Biol. 5 (2004) 214.
[5] A.W. Cohen, R. Hnasko, W. Schubert, M.P. Lisanti, Role of caveolae and caveolins in health and disease, Physiol. Rev. 84 (2004) 1341–1379.
[6] P.E. Fielding, J.S. Russel, T.A. Spencer, H. Hakamata, K. Nagao, C.J. Fielding, Sterol efflux to apolipoprotein A-I originates from caveolin-rich microdomains and potentiates PDGF-dependent protein kinase activity, Biochemistry 41 (2002) 4929–4937.
[7] P. Gargalovic, L. Dory, Cellular apoptosis is associated with increased caveolin-1 expression in macrophages, J. Lipid Res. 44 (2003) 1622–1632.
[8] P. Gargalovic, L. Dory, Caveolins and macrophage lipid metabolism, J. Lipid Res. 44 (2003) 11–21.
[9] P.U. Le, G. Guay, Y. Altschuler, I.R. Nabi, Caveolin-1 is a negative regulator of caveolae-mediated endocytosis to the endoplasmic reticulum, J. Biol. Chem. 277 (2002) 3371–3379.
[10] W.T. Chao, S.S. Fan, J.K. Chen, V.C. Yang, Visualizing caveolin-1 and HDL in cholesterol-loaded aortic endothelial cells, J. Lipid Res. 44 (2003) 1094–1099.
[11] Y. Fu, A. Hoang, G. Escher, R.G. Parton, Z. Krozowski, D. Sviridov, Expression of caveolin-1 enhances cholesterol efflux in hepatic cells, J. Biol. Chem. 279 (2004) 14140–14146.
[12] M. Sargiacomo, P.E. Scherer, Z. Tang, E. Kubler, K.S. Song, M.C. Sanders, M.P. Lisanti, Oligomeric structure of caveolin: implications for caveolae membrane organization, Proc. Natl. Acad. Sci. U. S. A. 92 (1995) 9407–9411.
[13] C. Mineo, G.L. James, E.J. Smart, R.G. Anderson, Localization of epidermal growth factor-stimulated Ras/Raf-1 interaction to caveolae membrane, J. Biol. Chem. 271 (1996) 11930–11935.
[14] P. Liu, Y. Ying, R.G. Anderson, Platelet-derived growth factor activates mitogen-activated protein kinase in isolated caveolae, Proc. Natl. Acad. Sci. U. S. A. 94 (1997) 13666–13670.
[15] F. Acconcia, P. Ascenzi, A. Bocedi, E. Spisni, V. Tomasi, A. Trentalance, P. Visca, M. Marino, Palmitoylation-dependent estrogen receptor alpha membrane localization: regulation by 17beta-estradiol, Mol. Biol. Cell 16 (2005) 231–237.
[16] B. Razani, M.P. Lisanti, Caveolin-deficient mice: insights into caveolar function and human disease, J. Clin. Invest. 108 (2001) 1553–1561.
[17] B. Razani, S.E. Woodman, M.P. Lisanti, Caveolae: from cell biology to animal physiology, Pharmacol. Rev. 54 (2002) 431–467.
[18] E. Spisni, C. Griffoni, S. Santi, M. Riccio, R. Marulli, G. Bartolini, M. Toni, V. Ullrich, V. Tomasi, Colocalization prostacyclin (PGI2) synthase-caveolin-1 in endothelial cells and new roles for PGI2 in angiogenesis, Exp. Cell Res. 266 (2001) 31–43.
[19] M.L. Massimino, C. Griffoni, E. Spisni, M. Toni, V. Tomasi, Involvement of caveolae and caveolae-like domains in signalling cell survival and angiogenesis, Cell. Signal. 14 (2002) 93–98.
[20] R.G. Parton, M. Hanzal-Bayer, J.F. Hancock, Biogenesis of caveolae: a structural model for caveolin-induced domain formation, J. Cell Sci. 119 (2006) 787–796.
[21] A.G. Ostermeyer, L.T. Ramcharan, Y. Zeng, D.M. Lunlin, D.A. Brown, Role of the hydrophobic domain in targeting caveolin-1 to lipid droplets, J. Cell Biol. 164 (2004) 69–78.
[22] S. Aoki, A. Thomas, M. Decaffmeyer, R. Brasseur, R.M. Epand, The role of proline in the membrane re-entrant helix of caveolin-1, J. Biol. Chem. 285 (2010) 33371–33380.
[23] A. Arbuzova, L. Wang, J. Wang, G. Hangyas-Mihalyne, D. Murray, B. Honig, S. McLaughlin, Membrane binding of peptides containing both basic and aromatic residues. Experimental studies with peptides corresponding to the scaffolding region of caveolin and the effector region of MARCKS, Biochemistry 39 (2000) 10330–10339.
[24] A. Schlegel, R.B. Schwab, P.E. Scherer, M.P. Lisanti, A role for the caveolin scaffolding domain in mediating the membrane attachment of caveolin-1—the caveolin scaffolding domain is both necessary and sufficient for membrane binding in vitro, J. Biol. Chem. 274 (1999) 22660–22667.
[25] A. Schlegel, M.P. Lisanti, A molecular dissection of caveolin-1 membrane attachment and oligomerization—two separate regions of the caveolin-1 C-terminal domain mediate membrane binding and oligomer/oligomer interactions in vivo, J. Biol. Chem. 275 (2000) 21605–21617.
[26] J. Couet, S. Li, T. Okamoto, T. Ikezu, M.P. Lisanti, Identification of peptide and protein ligands for the caveolin-scaffolding domain. Implications for the interaction of caveolin with caveolae-associated proteins, J. Biol. Chem. 272 (1997) 6525–6533.
[27] A.F. Quest, L. Leyton, M. Parraga, Caveolins, caveolae, and lipid rafts in cellular transport, signaling, and disease, Biochem. Cell Biol. 82 (2004) 129–144.
[28] T.M. Williams, M.P. Lisanti, Caveolin-1 in oncogenic transformation, cancer, and metastasis, Am. J. Physiol. Cell Physiol. 288 (2005) C494–C506.
[29] B.M. Collins, M.J. Davis, J.F. Hancock, R.G. Parton, Structure-based reassessment of the caveolin signaling model: do caveolae regulate signaling through caveolin–protein interactions? Dev. Cell 23 (2012) 11–20.
[30] S. Aoki, R.M. Epand, Caveolin-1 hydrophobic segment peptides insertion into membrane mimetic systems: role of Proline residue, Biochim. Biophys. Acta Biomembr. 1818 (2012) 12–18.
[31] J. Lee, K.J. Glover, The transmembrane domain of caveolin-1 exhibits a helix–break–helix structure, Biochim. Biophys. Acta Biomembr. 1818 (2012) 1158–1164.
[32] M.D. Rieth, J. Lee, K.J. Glover, Probing the caveolin-1 P132L mutant: critical insights into its oligomeric behaviour and structure, Biochemistry 51 (2012) 3911–3918.
[33] C.L. Hoop, V.N. Sivanandam, R. Kodali, M.N. Srnec, P.C.A. van der Wel, Structural characterization of the caveolin scaffolding domain in association with cholesterol-rich membranes, Biochemistry 51 (2012) 90–99.
[34] C. Le Lan, J.M. Neumann, N. Jamin, Role of the membrane interface on the conformation of the caveolin scaffolding domain: a CD and NMR study, FEBS Lett. 580 (2006) 5301–5305.
[35] M. Murata, J. Peranen, R. Schreiner, F. Wieland, T.V. Kurzchalia, K. Simons, VIP21/caveolin is a cholesterol-binding protein, Proc. Natl. Acad. Sci. U. S. A. 92 (1995) 10339–10343.
[36] S. Li, K.S. Song, M.P. Lisanti, Expression and characterization of recombinant caveolin. Purification by polyhistidine tagging and cholesterol-dependent incorporation into defined lipid membranes, J. Biol. Chem. 271 (1996) 568–573.
[37] E.J. Smart, Y. Ying, W.C. Donzell, R.G. Anderson, A role for caveolin in transport of cholesterol from endoplasmic reticulum to plasma membrane, J. Biol. Chem. 271 (1996) 29427–29435.
[38] A. Pol, R. Luetterforst, M. Lindsay, S. Heino, E. Ikonen, R.G. Parton, A caveolin dominant negative mutant associates with lipid bodies and induces intracellular cholesterol imbalance, J. Cell Biol. 152 (2001) 1057–1070.
[39] A. Gafencu, M. Stanescu, A.M. Toderici, C. Heltianu, M. Simionescu, Protein and fatty acid composition of caveolae from apical plasmalemma of aortic endothelial cells, Cell Tissue Res. 293 (1998) 101–110.
[40] D.W.L. Ma, J.M. Seo, L.A. Davidson, E.S. Callaway, Y.Y. Fan, J.R. Lupton, R.S. Chapkin, n−3 PUFA alter caveolae lipid composition and resident protein localization in mouse colon, FASEB J. 18 (2004) 1040–1042.
[41] P.S.P. Huot, B. Sarkar, D.W.L. Ma, Conjugated linoleic acid alters caveolae phospholipid fatty acid composition and decreases caveolin-1 expression in MCF-7 breast cancer cells, Nutr. Res. 30 (2010) 179–185.
[42] Q. Cai, L. Guo, H.Q. Gao, X.A. Li, Caveolar fatty acids and acylation of caveolin-1, Plos One 8 (2013) e60884.
[43] D.A. Brown, E. London, Structure and function of sphingolipid- and cholesterol-rich membrane rafts, J. Biol. Chem. 275 (2000) 17221–17224.
[44] A. Uittenbogaard, E.J. Smart, Palmitoylation of caveolin-1 is required for cholesterol binding, chaperone complex formation, and rapid transport of cholesterol to caveolae, J. Biol. Chem. 275 (2000) 25595–25599.
[45] D.J. Dietzen, W.R. Hastings, D.M. Lublin, Caveolin is palmitoylated on multiple cysteine residues. Palmitoylation is not necessary for localization of caveolin to caveolae, J. Biol. Chem. 270 (1995) 6838–6842.
[46] P.G. Frank, Y.L. Marcel, M.A. Connelly, D.M. Lublin, V. Franklin, D.L. Williams, M.P. Lisanti, Stabilization of caveolin-1 by cellular cholesterol and scavenger receptor class B type I, Biochemistry 41 (2002) 11931–11940.
[47] H. Li, V. Papadopoulos, Peripheral-type benzodiazepine receptor function in cholesterol transport. Identification of a putative cholesterol recognition/interaction amino acid sequence and consensus pattern, Endocrinology 139 (1998) 4991–4997.
[48] H. Li, Z.X. Yao, B. Degenhardt, G. Teper, V. Papadopoulos, Cholesterol binding at the cholesterol recognition/interaction amino acid consensus (CRAC) of the peripheral-type benzodiazepine receptor and inhibition of steroidogenesis by an HIV TAT-CRAC peptide, Proc. Natl. Acad. Sci. U. S. A. 98 (2001) 1267–1272.
[49] C. Le Lan, J. Gallay, M. Vincent, J.M. Neumann, B. de Foresta, N. Jamin, Structural and dynamic properties of juxta-membrane segments of caveolin-1 and caveolin-2 at the membrane interface, Eur. Biophys. J. 39 (2010) 307–325.
[50] S.E. Woodman, A. Schlegel, A.W. Cohen, M.P. Lisanti, Mutational analysis identifies a short atypical membrane attachment sequence (KYWFYR) within caveolin-1, Biochemistry 41 (2002) 3790–3795.
[51] R.M. Epand, B.G. Sayer, R.F. Epand, Peptide-induced formation of cholesterol-rich domains, Biochemistry 42 (2003) 14677–14689.
[52] R.M. Epand, B.G. Sayer, R.F. Epand, Caveolin scaffolding region and cholesterol-rich domains in membranes, J. Mol. Biol. 345 (2005) 339–350.
[53] F. Cunningham, C.M. Deber, Optimizing synthesis and expression of transmembrane peptides and proteins, Methods 41 (2007) 370–380.
[54] R.N. Lewis, N. Mak, R.N. McElhaney, A differential scanning calorimetric study of the thermotropic phase behaviour of model membranes composed of phosphatidylcholines containing linear saturated fatty acyl chains, Biochemistry 26 (1987) 6118–6126.
[55] H. Ichimori, T. Hata, H. Matsuki, S. Kaneshina, Barotropic phase transitions and pressure-induced interdigitation on bilayer membranes of phospholipids with varying acyl chain lengths, Biochim. Biophys. Acta 1414 (1998) 165–174.
[56] T.P. McMullen, R.N. McElhaney, New aspects of the interaction of cholesterol with dipalmitoylphosphatidylcholine bilayers as revealed by high-sensitivity differential scanning calorimetry, Biochim. Biophys. Acta 1234 (1995) 90–98.

[57] A. Morisco, A. Accardo, E. Gianolio, D. Tesauro, E. Benedetti, G. Morelli, Micelles derivatized with octreotide as potential target-selective contrast agents in MRI, J. Pept. Sci. 15 (2009) 242–250.
[58] P.O. Freskgard, L.G. Martensson, P. Jonasson, B.H. Jonsson, U. Carlsson, Assignment of the contribution of the tryptophan residues to the circular dichroism spectrum of human carbonic anhydrase II, Biochemistry 33 (1994) 14281–14288.
[59] R.I. Saba, J.-M. Ruysschaert, A. Herchuelz, E. Goormaghtigh, Fourier transform infrared spectroscopy study of the secondary and tertiary structure of the reconstituted Na^{+}/Ca^{2+} exchanger 70-kDa polypeptide, J. Biol. Chem. 274 (1999) 15510–15518.
[60] R.M. Epand, Proteins and cholesterol-rich domains, Biochim. Biophys. Acta Biomembr. 1778 (2008) 1576–1582.
[61] R.M. Epand, Do proteins facilitate the formation of cholesterol-rich domains? Biochim. Biophys. Acta Biomembr. 1666 (2004) 227–238.
[62] J.H. Ipsen, G. Karlstrom, O.G. Mouritsen, H. Wennerstrom, M.J. Zuckermann, Phase equilibria in the phosphatidylcholine–cholesterol system, Biochim. Biophys. Acta 905 (1987) 162–172.
[63] N. Tamai, T. Izumikawa, S. Fukui, M. Uemura, M. Goto, H. Matsuki, S. Kaneshina, How does acyl chain length affect thermotropic phase behaviour of saturated diacylphosphatidylcholine–cholesterol binary bilayers? Biochim. Biophys. Acta Biomembr. 1828 (2013) 2513–2523.
[64] T. Harder, K. Simons, Caveolae, DIGs, and the dynamics of sphingolipid–cholesterol microdomains, Curr. Opin. Cell Biol. 9 (1997) 534–542.
[65] Y.H. Hao, J.W. Chen, Influence of cholesterol on the biophysical properties of the sphingomyelin/DOPC binary system, J. Membr. Biol. 183 (2001) 85–92.